

Universal dimer-dimer scattering in lattice effective field theory

Serdar Elhatisari,^{1,2,*} Kris Katterjohn,^{3,†} Dean Lee,^{4,‡}
Ulf-G. Meißner,^{1,5,§} and Gautam Rupak^{3,¶}

¹*Helmholtz-Institut für Strahlen- und Kernphysik (Theorie)
and Bethe Center for Theoretical Physics, Universität Bonn, D-53115 Bonn, Germany*

²*Department of Physics, Karamanoglu Mehmetbey University, Karaman 70100, Turkey*

³*Department of Physics & Astronomy and HPC² Center for Computational Sciences,
Mississippi State University, Mississippi State, Mississippi State 39762, USA*

⁴*Department of Physics, North Carolina State University,
Raleigh, North Carolina 27695, USA*

⁵*Institute for Advanced Simulation, Institut für Kernphysik,
Jülich Center for Hadron Physics and JARA - High Performance Computing,
Forschungszentrum Jülich, D-52425 Jülich, Germany*

(Dated: June 26, 2021)

Abstract

We consider two-component fermions with short-range interactions and large scattering length. This system has universal properties that are realized in several different fields of physics. In the limit of large fermion-fermion scattering length a_{ff} and zero-range interaction, all properties of the system scale proportionally with a_{ff} . For the case with shallow bound dimers, we calculate the dimer-dimer scattering phase shifts using lattice effective field theory. We extract the universal dimer-dimer scattering length $a_{\text{dd}}/a_{\text{ff}} = 0.618(30)$ and effective range $r_{\text{dd}}/a_{\text{ff}} = -0.431(48)$. This result for the effective range is the first calculation with quantified and controlled systematic errors. We also benchmark our methods by computing the fermion-dimer scattering parameters and testing some predictions of conformal scaling of irrelevant operators near the unitarity limit.

* elhatisari@hiskp.uni-bonn.de

† kk278@msstate.edu

‡ dean.lee@ncsu.edu

§ meissner@hiskp.uni-bonn.de

¶ grupak@u.washington.edu

I. INTRODUCTION

Two-component fermions at large scattering length are an important system with universal properties and relevance to several branches of physics. This universality is due to the existence of a conformal fixed point called the unitarity limit where the fermion-fermion scattering length is infinite and all other length scale are irrelevant at large particle separations or low energies. See for example Ref. [1] for a review. In nuclear physics, the neutron-neutron scattering length $|a_{nn}| \sim 19$ fm [2] is much larger than the inverse pion mass $1/M_\pi \sim 1.4$ fm characterizing the exponential tail of the nuclear force. In the physics of ultracold atoms, one can tune the interactions arbitrarily close to the unitarity limit using an external magnetic field near a Feshbach resonance [3, 4]. In this letter we discuss the case where the scattering length is large and positive, and bound dimers composed of two fermions are formed with shallow binding energy. We compute dimer-dimer scattering and determine the the dimer-dimer scattering length and effective range. These results can be used to compute the energy density of a dimer gas in the dilute limit [5–9].

The elastic scattering phase shift $\delta(p)$ between two non-relativistic fermions with finite-range interactions is parameterized by the effective range expansion (ERE) [11],

$$p \cot \delta = -\frac{1}{a_{\text{ff}}} + \frac{1}{2} r_{\text{ff}} p^2 + \mathcal{O}(p^4), \quad (1)$$

where p is the relative momentum, a_{ff} is the fermion-fermion scattering length, and r_{ff} is the fermion-fermion effective range. In this study we consider the case where a_{ff} is large and positive while all other lengths scales are negligible. We can express all physical quantities in dimensionless combinations involving powers of a_{ff} . Previous calculations of the dimer-dimer scattering length have found $a_{\text{dd}}/a_{\text{ff}} = 0.60 \pm 0.01$ [14, 15], $a_{\text{dd}}/a_{\text{ff}} = 0.605 \pm 0.005$ [16], and $a_{\text{dd}}/a_{\text{ff}} = 0.60$ [17]. A perturbative expansion about four spatial dimensions gives $a_{\text{dd}}/a_{\text{ff}} \approx 0.66$ [18], and a rough estimate using the resonating group method in the single-channel approximation gives $a_{\text{dd}}/a_{\text{ff}} \sim 0.752$ [19]. On the other hand, much less is known about the higher-order dimer-dimer ERE parameters. The effective range has been calculated as $r_{\text{dd}}/a_{\text{ff}} \approx 0.12$ in Ref. [20], while a very rough estimate of $r_{\text{dd}}/a_{\text{ff}} \sim 2.6$ was given in Ref. [21].

In this work we calculate the low-energy dimer-dimer phase shifts from lattice effective field theory and extract both the dimer-dimer scattering length a_{dd} and effective range r_{dd} . We also benchmark our methods by calculating the fermion-dimer scattering length a_{fd} and effective range r_{fd} . We organize our paper as follows. In Sec. II we introduce the continuum and lattice formulations for systems of two-component fermions. In Sec. III we discuss the methods for extracting the scattering information from periodic finite volumes. We present our results and analyses for fermion-dimer and dimer-dimer scattering in Sec. IV. The results are summarized in Sec. V.

II. LATTICE FORMALISM

Following Refs. [22, 23], we start by describing interacting two-component fermions in continuous space. Low-energy fermion-fermion scattering is dominated by the s -wave channel, while higher partial waves become more important at higher energies. In principle the two components could have different masses, however we only consider the equal mass case in this study and denote the two components as up and down spins. We will consider systems of two-component fermions with different masses in a future publication.

We work with natural units where $\hbar = 1 = c$. Let $b_{\uparrow,\downarrow}$ ($b_{\uparrow,\downarrow}^\dagger$) be the annihilation (creation) operators, and let $\rho_{\uparrow,\downarrow}$ be the density operators,

$$\rho_{\uparrow}(\vec{r}) = b_{\uparrow}^\dagger(\vec{r})b_{\uparrow}(\vec{r}), \quad \rho_{\downarrow}(\vec{r}) = b_{\downarrow}^\dagger(\vec{r})b_{\downarrow}(\vec{r}). \quad (2)$$

The continuum Hamiltonian has the form

$$H = \sum_{s=\uparrow,\downarrow} \frac{1}{2m} \int d^3\vec{r} \vec{\nabla} b_s^\dagger(\vec{r}) \cdot \vec{\nabla} b_s(\vec{r}) + C_0 \int d^3\vec{r} \rho_{\uparrow}(\vec{r})\rho_{\downarrow}(\vec{r}), \quad (3)$$

where ultraviolet divergences due to the zero-range interaction are regulated in some manner. In our case we use the lattice to provide the ultraviolet regularization.

We denote the lattice spacing as a . In our calculations we use an $\mathcal{O}(a^4)$ -improved lattice action where the free lattice Hamiltonian, H_0 , is defined as,

$$H_0 = \sum_{s=\uparrow,\downarrow} \frac{1}{2m} \sum_{\hat{l}=\hat{1},\hat{2},\hat{3}} \sum_{\vec{n}} \left[\sum_{k=-3}^3 w_{|k|} b_s^\dagger(\vec{n}) b_s(\vec{n} + k\hat{l}) \right], \quad (4)$$

where $\hat{l} = \hat{1}, \hat{2}, \hat{3}$ are unit vectors in spatial directions, and the hopping parameters w_0, w_1, w_2 , and w_3 are $49/18, -3/2, 3/20$, and $-1/90$, respectively. \vec{n} denotes the lattice sites on a three-dimensional $L \times L \times L$ periodic cube.

For the two-particle ($2N$) interaction we use the single-site interaction

$$V_{2N} = C_{2N} \sum_{\vec{n}} \rho_{\uparrow}(\vec{n}) \rho_{\downarrow}(\vec{n}), \quad (5)$$

where the value of C_{2N} depends on the lattice spacing a . We tune C_{2N} to produce the desired value of the dimer binding energy B_d . For convenience we choose parameters typical for nuclear physics, with fermion mass $m = 939$ MeV and dimer binding energies ranging from 1 MeV to 10 MeV. However the final results are completely independent of these details when expressed in terms of the two-fermion scattering length a_{ff} .

In the low-energy limit of this theory, three-particle and higher-particle interactions are irrelevant operators. Nevertheless, we find it useful to include three-particle ($3N$) and four-particle ($4N$) interactions as a diagnostic tool to generate more data for the continuum-limit extrapolations. The three-particle interaction we use features nearest-neighbour and next-to-nearest-neighbour interactions,

$$\begin{aligned} V_{3N} = & C_{3N}^{(1)} \sum_{\vec{n}} \sum_{|\vec{n}-\vec{n}'|=1} \rho_{\uparrow}(\vec{n}) \rho_{\downarrow}(\vec{n}) [\rho_{\uparrow}(\vec{n}') + \rho_{\downarrow}(\vec{n}')] \\ & + C_{3N}^{(2)} \sum_{\vec{n}} \sum_{|\vec{n}-\vec{n}'|=2} \rho_{\uparrow}(\vec{n}) \rho_{\downarrow}(\vec{n}) [\rho_{\uparrow}(\vec{n}') + \rho_{\downarrow}(\vec{n}')]. \end{aligned} \quad (6)$$

Similarly, we introduce a four-particle interaction that consists of nearest-neighbour and next-to-nearest-neighbour interactions,

$$\begin{aligned} V_{4N} = & C_{4N}^{(1)} \sum_{\vec{n}} \sum_{|\vec{n}-\vec{n}'|=1} \rho_{\uparrow}(\vec{n}) \rho_{\downarrow}(\vec{n}) \rho_{\uparrow}(\vec{n}') \rho_{\downarrow}(\vec{n}') \\ & + C_{4N}^{(2)} \sum_{\vec{n}} \sum_{|\vec{n}-\vec{n}'|=2} \rho_{\uparrow}(\vec{n}) \rho_{\downarrow}(\vec{n}) \rho_{\uparrow}(\vec{n}') \rho_{\downarrow}(\vec{n}'). \end{aligned} \quad (7)$$

We keep the interaction strengths $C_{3N}^{(1,2)}$ and $C_{4N}^{(1,2)}$ at fixed values when measured in lattice units.

We can compute the importance of these irrelevant operators in the continuum limit near the conformally-invariant point where the two-fermion scattering length is infinite and the interaction range is zero. If δ is the scaling dimension of an operator O , then the contribution from the insertion of the interaction $O^\dagger O$ scales as $a^{2\delta-d-2}$ in the continuum limit, where d is the number of spatial dimensions [24]. The operator-state correspondence principle connects the scaling dimension of an operator to the lowest energy of the system in a harmonic trap with the corresponding number of particles and quantum numbers [25]. From numerical calculations of the harmonically-trapped energies, we deduce that the leading behavior of the three-particle operators is $a^{3.54544}$, while the leading behavior of the four-particle operators is $a^{5.056}$ [24]. In our analysis we will check explicitly if this dependence on the lattice spacing can be seen in the lattice results.

III. SCATTERING PHASE SHIFT

Lüscher's finite-volume method relates the two-body energy levels in a cubic periodic box to the elastic scattering phase shifts [26, 27]. The two-body phase shifts in a periodic box of size L are related to the relative momentum of the two bodies, p , by the relation

$$p \cot \delta(p) = \frac{1}{\pi L} S(\eta), \quad \eta = \left(\frac{pL}{2\pi} \right)^2, \quad (8)$$

where $S(\eta)$ is the regulated three-dimensional zeta function given by

$$S(\eta) = \lim_{\Lambda \rightarrow \infty} \left[\sum_{\vec{n}} \frac{\Theta(\Lambda^2 - \vec{n}^2)}{\vec{n}^2 - \eta} - 4\pi\Lambda \right]. \quad (9)$$

The sum in Eq. (9) is over three-dimensional integer vectors \vec{n} .

We use the Lanczos eigenvector method [28] to compute the low-energy spectrum of the lattice Hamiltonian at different values of L . These energies levels determine the values of p as input into Eq. (8), which then determine the two-body scattering phase shifts $\delta(p)$. First we do these calculations for the three-particle system to determine the fermion-dimer scattering parameters. We then do the calculations for the four-particle system to determine the dimer-dimer scattering parameters.

In the zero-range limit, the fermion-fermion scattering length is related to the dimer binding energy by the formula

$$B_d = \frac{1}{ma_{\text{ff}}^2}. \quad (10)$$

Since we will take the zero-range limit in all our calculations, we can define a_{ff} quite simply using the zero-range formula in Eq. (10) and the dimer binding energy B_d determined on the lattice. However, we can also determine the fermion-fermion scattering length more carefully using Lüscher's finite-volume scattering method. We call this determination of the scattering length a_{ff}^* . In Fig. 1 we show the ratio of the scattering lengths for various lattice spacings a . In the plot we have fitted a polynomial in a/a_{ff} to the results. We see that the deviation between these two definitions of the scattering length vanishes in the continuum limit and can be fit well by a polynomial in a/a_{ff} .

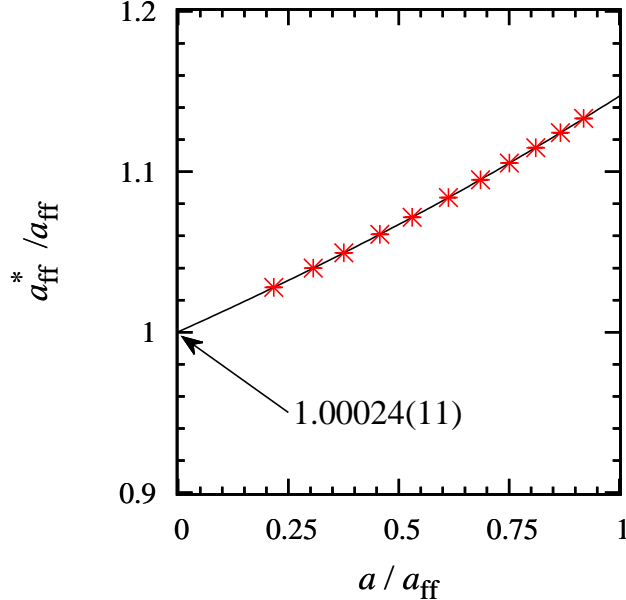


FIG. 1: The ratio of the fermion-fermion scattering length a_{ff}^* determined using Lüscher’s finite volume formula and a_{ff} determined from B_{d} . The results are plotted versus the lattice spacing a as a fraction of a_{ff} , and fitted to a polynomial in a/a_{ff} .

We will use Lüscher’s finite-volume method to calculate fermion-dimer scattering and dimer-dimer scattering. In these cases we consider the scattering of two bodies, where one or both bodies may be dimers. Let μ_{12} be the reduced mass of the two scattering objects. In the infinite volume and continuum limits, the relative momentum p is related to the two-body energy level $E^{(\infty)}$ as

$$E^{(\infty)} = \frac{p^2}{2\mu_{12}} - B_1 - B_2, \quad (11)$$

where B_1 and B_2 are the infinite-volume binding energies for the two bodies. These will equal B_{d} if a dimer or 0 if a fermion.

Eq. (11) is modified by several effects at finite volume and nonzero lattice spacing. At nonzero lattice spacing, the effective mass of the dimer is not exactly equal to twice the fermion mass. So we numerically calculate the energy versus momentum dispersion relation of the dimer to extract the dimer effective mass. For this we use a large $L = 50a$ cubic box in order to minimize finite-volume errors. From the dimer effective mass we can determine the reduced mass of the fermion-dimer and dimer-dimer systems. We write this lattice-determined reduced mass as μ_{12}^* .

At finite volume, there is also a finite-volume correction to the binding energies B_1 and B_2 . These finite-volume corrections vanish exponentially with the size of the box and so can be ignored for sufficiently large L . However computational limits often make very large volume calculations impractical, and it so is useful to remove finite-volume corrections corresponding to binding energies when possible. It turns out that the finite-volume corrections to the binding energies B_1 and B_2 are momentum dependent. We account for these finite-volume momentum-dependent effects using finite-volume topological factors $\tau(\eta)$ due to the dimer wave functions wrapping around the periodic box [29], where η was defined in Eq. (8). With

these corrections, Eq. (11) becomes

$$E^{(L)} = \frac{p^2}{2\mu_{12}^*} - B_1 - \tau_1(\eta) \Delta B_1^{(L)} - B_2 - \tau_2(\eta) \Delta B_2^{(L)}, \quad (12)$$

where $\Delta B_i^{(L)}$ is the finite-volume correction $\Delta B_i^{(L)} = B_i^{(L)} - B_i$. The topological factor is given by [29]

$$\tau(\eta) = \left[\sum_{\vec{k}} \frac{1}{(\vec{k}^2 - \eta)^2} \right]^{-1} \sum_{\vec{k}} \frac{\sum_{i=1}^3 \cos(2\pi\alpha k_i)}{3(\vec{k}^2 - \eta)^2}, \quad (13)$$

where \vec{k} runs over all integer vectors, and $\alpha = 1/2$ for the dimer bound state. The relative momentum p corresponding to box length L is computed by solving Eq. (12) self-consistently for the given lattice energies $E^{(L)}$, $B_{1,2}^{(L)}$, and $B_{1,2}$.

IV. RESULTS AND ANALYSIS

A. Fermion-dimer scattering

Before proceeding to the dimer-dimer system, we perform benchmarks of our lattice methods and analysis by computing fermion-dimer scattering. Fermion-dimer scattering has been calculated using semi-analytical methods [12, 30–32] in the continuum limit. We consider a three-particle system of two spin-up fermions and one spin-down fermion. Our lattice Hamiltonian has the form

$$H = H_0 + V_{2N} + V_{3N}, \quad (14)$$

where the free Hamiltonian is defined in Eq. (4), the two-particle interaction appears in Eq. (5), and the three-particle interaction is introduced in Eq. (6). In order to reduce the number of free parameters in our analysis, we define the three-particle parameter c_{3N} and set $C_{3N}^{(1)} = c_{3N}$ and $C_{3N}^{(2)} = c_{3N}/2$. In the following we quote the value of c_{3N} in lattice units.

We perform lattice calculations using the Lanczos eigenvector method to obtain the finite-volume energies of the fermion-dimer system for various interaction coefficients C_{2N} and c_{3N} and lattice lengths L . From the fermion-dimer energies $E_{\text{fd}}^{(L)}$ in the center-of-mass frame, we determine the relative momentum p using

$$E_{\text{fd}}^{(L)} = \frac{p^2}{2\mu_{\text{fd}}^*} - B_{\text{d}} - \tau_{\text{d}}(\eta) \Delta B_{\text{d}}^{(L)}, \quad (15)$$

and then use Eq. (8) to extract the fermion-dimer scattering phase shifts.

The results for the fermion-dimer phase shifts are shown in Fig. 2. We plot $a_{\text{ff}} p \cot \delta$ versus $(a_{\text{ff}} p)^2$ for various values of the three-particle coupling c_{3N} and various ratios of the lattice spacing a to the fermion-fermion scattering length a_{ff} . The values quoted for c_{3N} are in lattice units. In each case we make a fit using the truncated effective range expansion

$$a_{\text{ff}} p \cot \delta = -\frac{1}{a_{\text{fd}}/a_{\text{ff}}} + \frac{1}{2} r_{\text{fd}}/a_{\text{ff}} \cdot (a_{\text{ff}} p)^2 + O(p^4), \quad (16)$$

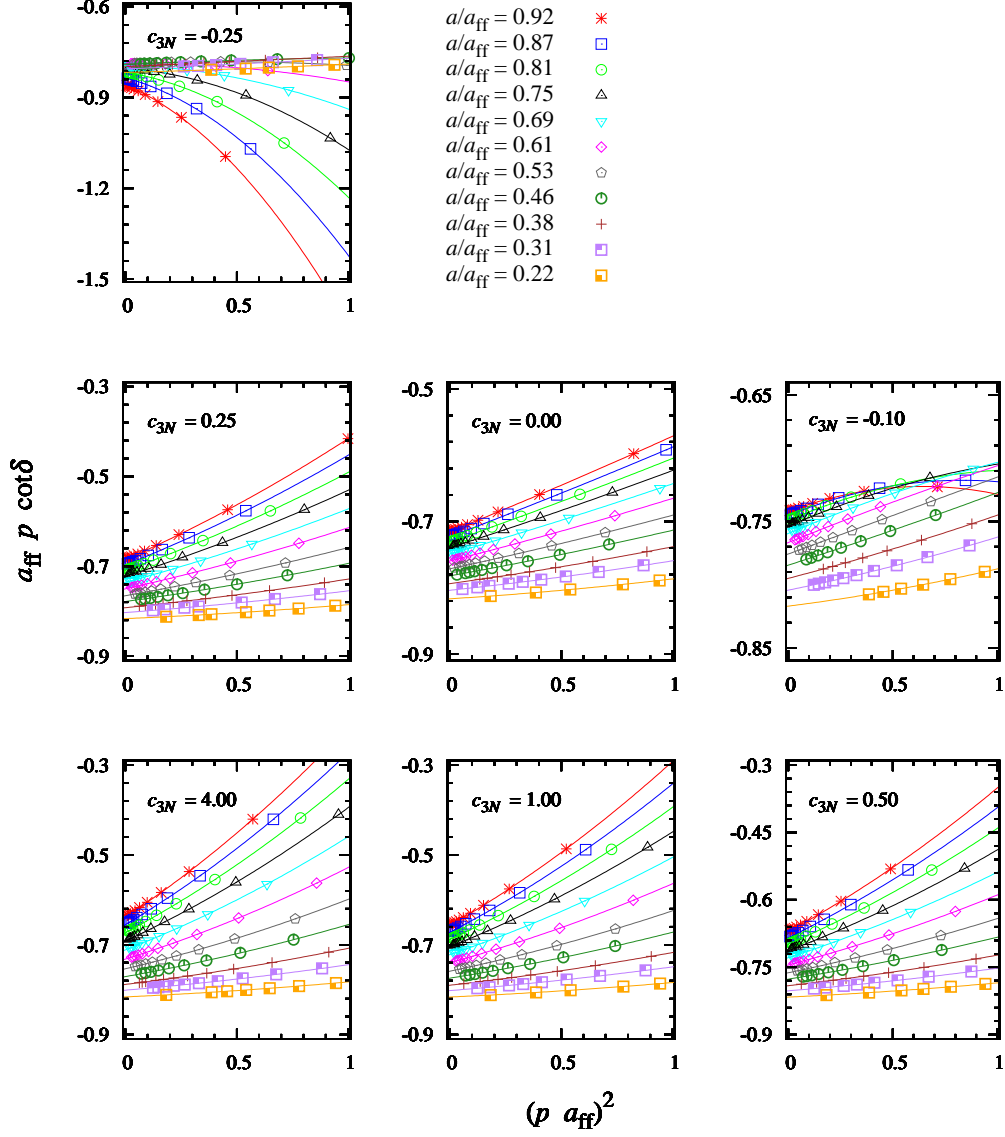


FIG. 2: The fermion-dimer scattering results for various values of the three-particle coupling c_{3N} in lattice units and various ratios of the lattice spacing a to the fermion-fermion scattering length a_{ff} . We plot $a_{\text{ff}} p \cot \delta$ versus $(a_{\text{ff}} p)^2$ in the center-of-mass frame. The points are the lattice data, and the lines are the fits to the effective range expansion.

where a_{fd} and r_{fd} are the fermion-dimer scattering length and effective range respectively. As seen in Fig. 2, the three-particle interactions have some impact on the scattering phase shift results at larger lattice spacings, while the data at small a is almost independent of c_{3N} . This is consistent with the conformal scaling prediction that the three-particle interactions are irrelevant in the continuum limit.

With these lattice results for a_{fd} and r_{fd} , we extrapolate to the continuum limit. There will be lattice cutoff corrections that scale as integer powers of the lattice spacing. For these corrections we fit a third-order polynomial in a/a_{ff} with coefficients that are independent of c_{3N} . We also include the predicted leading order correction from c_{3N} as $(a/a_{\text{ff}})^{3.54544}$ as well as a subleading correction at one power higher, $(a/a_{\text{ff}})^{4.54544}$. We could include other corrections as well, however there is a limit to the number of powers that can be fit reliably

at the same time. In summary, we perform the continuum-limit extrapolations for a_{fd} and r_{fd} using the functional form

$$f(a/a_{\text{ff}}) = f_0 + f_1 (a/a_{\text{ff}}) + f_2 (a/a_{\text{ff}})^2 + f_3 (a/a_{\text{ff}})^3 + f_{3.54544} (a/a_{\text{ff}})^{3.54544} + f_{4.54544} (a/a_{\text{ff}})^{4.54544}, \quad (17)$$

where f_0, f_1, f_2 , and f_3 are independent of c_{3N} while $f_{3.54544}$ and $f_{4.54544}$ depend on c_{3N} .

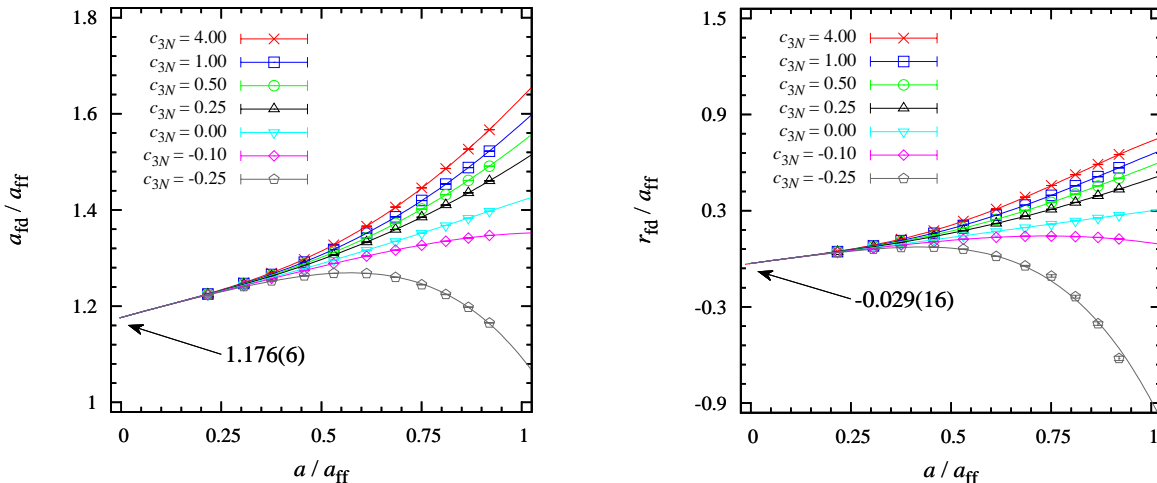


FIG. 3: (Left panel) The continuum-limit extrapolation of the fermion-dimer scattering length a_{fd} . (Right panel) The continuum-limit extrapolation of the fermion-dimer effective range r_{fd} . The final results are $a_{\text{fd}}/a_{\text{ff}} = 1.176(6)$ and $r_{\text{fd}}/a_{\text{ff}} = -0.029(16)$.

The extrapolation fits for the scattering length and the effective range are shown in Fig. 3. The final results for the scattering parameters are $a_{\text{fd}}/a_{\text{ff}} = 1.176(6)$ and $r_{\text{fd}}/a_{\text{ff}} = -0.029(16)$, which are in good agreement with semi-analytic continuum calculations $a_{\text{fd}}^{\text{cont.}}/a_{\text{ff}} = 1.1791(2)$ and $r_{\text{fd}}^{\text{cont.}}/a_{\text{ff}} = -0.0383(3)$ [12, 30–32]. The error bars include the uncertainty from the effective range expansion fits and the continuum limit extrapolation. Given the quality of the extrapolation fits in Fig. 3, we conclude that the three-particle forces make a contribution that is consistent with the conformal scaling prediction of $(a/a_{\text{ff}})^{3.54544}$.

B. Dimer-dimer scattering

We now compute dimer-dimer scattering. We consider a four-particle system of two spin-up fermions and two spin-down fermions. Our lattice Hamiltonian has the form

$$H = H_0 + V_{2N} + V_{3N} + V_{4N}, \quad (18)$$

where the four-particle interaction is introduced in Eq. (7). For our analysis we define the parameter $c_{3N,4N}$ and set $C_{3N}^{(1)} = 2C_{3N}^{(2)} = c_{3N,4N}$ and $C_{4N}^{(1)} = 2C_{4N}^{(2)} = -3c_{3N,4N}$. In the following we quote the value of $c_{3N,4N}$ in lattice units.

As in the fermion-dimer calculations, we use the Lanczos eigenvector method to obtain the finite-volume energies for the dimer-dimer system for various interaction coefficients C_{2N}

and $c_{3N,4N}$ and lattice lengths L . From the dimer-dimer energies $E_{\text{dd}}^{(L)}$ in the center-of-mass frame, we determine the relative momentum p using

$$E_{\text{dd}}^{(L)} = \frac{p^2}{2\mu_{\text{dd}}^*} - 2B_{\text{d}} - 2\tau_{\text{d}}(\eta) \Delta B_{\text{d}}^{(L)}, \quad (19)$$

and then use Eq. (8) to extract the dimer-dimer scattering phase shifts.

The results for the dimer-dimer phase shifts are shown in Fig. 4. We plot $a_{\text{ff}} p \cot \delta$ versus $(a_{\text{ff}} p)^2$ for various values of the multi-particle coupling $c_{3N,4N}$ and various ratios of the lattice spacing a to the fermion-fermion scattering length a_{ff} . The values quoted for $c_{3N,4N}$ are in lattice units. In each case we make a fit using the truncated effective range expansion

$$a_{\text{ff}} p \cot \delta = -\frac{1}{a_{\text{dd}}/a_{\text{ff}}} + \frac{1}{2} r_{\text{dd}}/a_{\text{ff}} \cdot (a_{\text{ff}} p)^2 + O(p^4), \quad (20)$$

where a_{dd} and r_{dd} are the dimer-dimer scattering length and effective range respectively. We observe in Fig. 4 that the multi-particle coupling $c_{3N,4N}$ has a stronger impact on the dimer-dimer scattering results than we had seen for c_{3N} in the fermi-dimer scattering results. This is due to finite-volume effects. It is not possible at present to go to very large volumes in the four-particle system calculations. The amount of memory required scales as ℓ^9 , where $\ell = L/a$ is the lattice length measured in lattice units. In practice it is difficult to go much beyond $\ell = 12$. This is in contrast with the three-particle system where the scaling is as ℓ^6 , and one can reach values of ℓ several times larger.

In the absence of the multi-particle coupling $c_{3N,4N}$, we find that the finite-volume corrections for the four-particle system are significant. These findings are consistent with Ref. [34], which discussed a four-particle chain-like excitation wrapping around the lattice boundaries. In addition to the leading $(a/a_{\text{ff}})^{3.54544}$ dependence on $c_{3N,4N}$, we also have corrections proportional to $(a/a_{\text{ff}})^{3.54544}$ times a term proportional to the finite-volume correction of the dimer wave function [33],

$$(a/a_{\text{ff}})^{3.54544} \frac{e^{-L/a_{\text{ff}}}}{L/a_{\text{ff}}}. \quad (21)$$

Written in terms of ℓ , this becomes

$$(a/a_{\text{ff}})^{3.54544} \frac{e^{-\ell a/a_{\text{ff}}}}{\ell a/a_{\text{ff}}} = (a/a_{\text{ff}})^{2.54544} \frac{e^{-\ell a/a_{\text{ff}}}}{\ell}, \quad (22)$$

and so for fixed ℓ we get a correction that naïvely appears to be of a lower order than the expected $(a/a_{\text{ff}})^{3.54544}$ scaling and with a rather complicated dependence on a/a_{ff} . Even though this dependence on a/a_{ff} is an artificial combination of lattice and finite volume effects, we can still extrapolate the lattice data to obtain the correct continuum limit.

In light of the complications from residual finite-volume effects, we use a simpler continuum extrapolation scheme for a_{dd} and r_{dd} . For a_{dd} we use a simple functional form

$$f(a/a_{\text{ff}}) = f_0 + f_1 (a/a_{\text{ff}}) + f_2 (a/a_{\text{ff}})^2 + f_3 (a/a_{\text{ff}})^3 \quad (23)$$

with f_0 independent of $c_{3N,4N}$, but allowing f_1 , f_2 , and f_3 to vary with $c_{3N,4N}$. In Fig. 5 we show the continuum-limit extrapolation for the dimer-dimer scattering length a_{dd} . The final result we obtain is $a_{\text{dd}}/a_{\text{ff}} = 0.618(30)$, which is in good agreement with the most accurate determinations in the literature, $a_{\text{dd}}/a_{\text{ff}} = 0.60 \pm 0.01$ [14, 15], $a_{\text{dd}}/a_{\text{ff}} = 0.605 \pm 0.005$ [16],

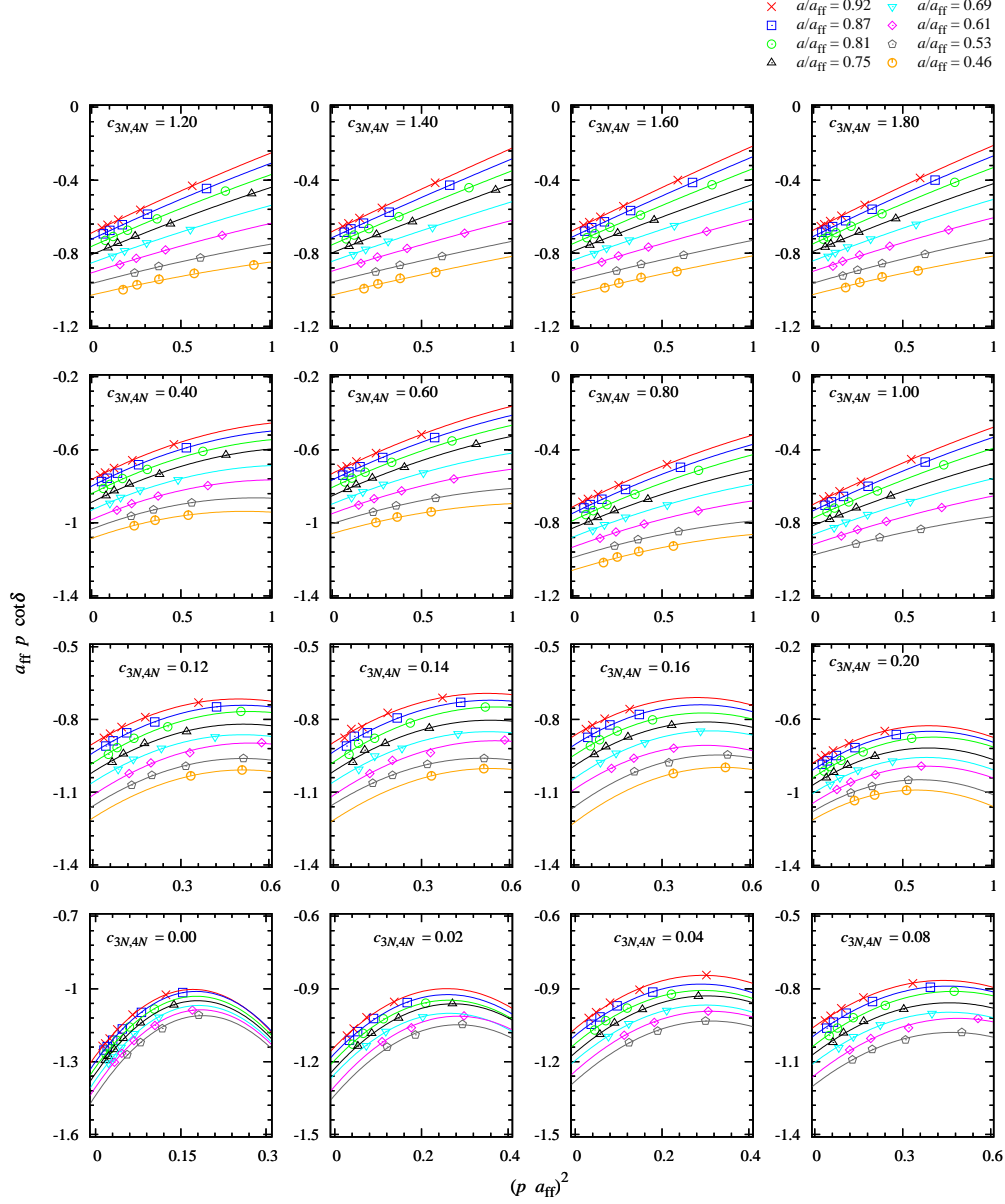


FIG. 4: The dimer-dimer scattering results for various values of the multi-particle coupling $c_{3N,4N}$ in lattice units and various ratios of the lattice spacing a to the fermion-fermion scattering length a_{ff} . We plot $a_{\text{ff}} p \cot \delta$ versus $(a_{\text{ff}} p)^2$ in the center-of-mass frame. The points are the lattice data, and the lines are the fits to the effective range expansion.

and $a_{\text{dd}}/a_{\text{ff}} = 0.60$ [17]. The error bar includes the uncertainty from the effective range expansion fits and the continuum limit extrapolation.

As we increase $c_{3N,4N}$, the three-particle interaction becomes more repulsive. This repulsive interaction impedes the formation of the chain-like excitation wrapping around the periodic boundary which was observed in Ref. [34]. So the finite-volume corrections are smaller for large positive values of $c_{3N,4N}$, and we expect to recover the usual $(a/a_{\text{ff}})^{3.54544}$ dependence on $c_{3N,4N}$. This is consistent with the results in Fig. 5. For the largest values of $c_{3N,4N}$, the coefficients of the first and second powers of a/a_{ff} are approximately independent of $c_{3N,4N}$.

For the continuum extrapolation of r_{dd} , we use only the data with $c_{3N,4N} \geq 0.40$, where the three-particle interaction is quite repulsive and finite-volume effects are small. We use the functional form

$$f(a/a_{\text{ff}}) = f_0 + f_1 (a/a_{\text{ff}}) + f_2 (a/a_{\text{ff}})^2 \quad (24)$$

with f_0 independent of $c_{3N,4N}$, but allowing f_1 and f_2 to vary with $c_{3N,4N}$. In Fig. 6 we show the continuum-limit extrapolation for the dimer-dimer effective range r_{dd} . We note that as $c_{3N,4N}$ increases, the coefficients of the first and second powers of a/a_{ff} are approximately independent of $c_{3N,4N}$. This is consistent with the expected $(a/a_{\text{ff}})^{3.54544}$ dependence on $c_{3N,4N}$. The final result we obtain is $r_{\text{dd}}/a_{\text{ff}} = -0.431(48)$. The error bar includes the uncertainty from the effective range expansion fits and the continuum limit extrapolation. This value is different from previous estimates in the literature, $r_{\text{dd}}/a_{\text{ff}} \approx 0.12$ [20] and $r_{\text{dd}}/a_{\text{ff}} \sim 2.6$ [21]. However in each of the previous estimates, the size of the systematic errors have not been quantified. In particular the analysis in Ref. [21] was plagued by the same large finite-volume effects we have discussed here. In our analysis we used the repulsive three-particle interaction to reduce the size of the finite-volume corrections.

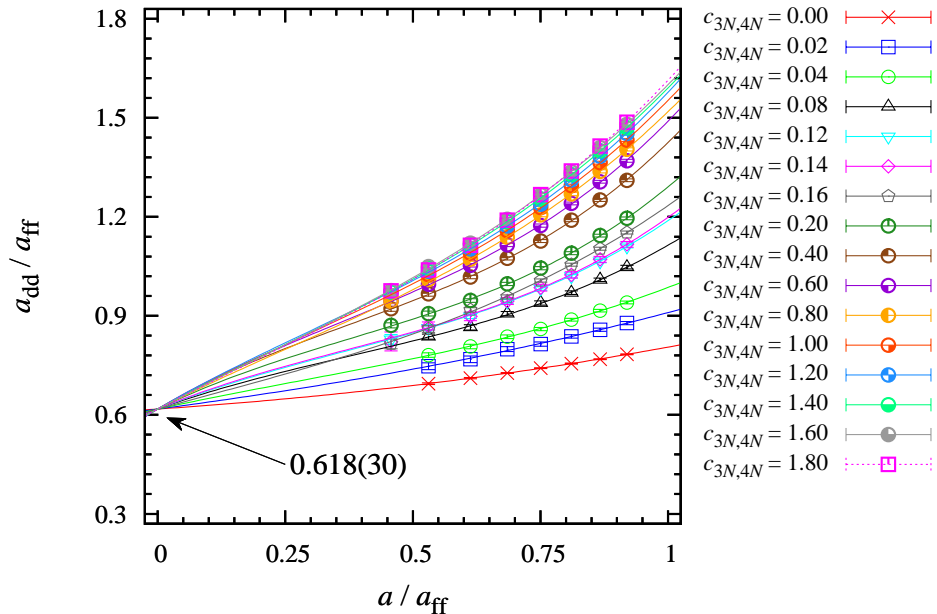


FIG. 5: The continuum-limit extrapolation of the dimer-dimer scattering length a_{dd} . The final result is $a_{\text{dd}}/a_{\text{ff}} = 0.618(30)$.

To further analyze the sign of the effective range, we have considered a simple model of the dimer-dimer system consisting of two fundamental particles. Due to the Pauli repulsion between identical particles, it is very plausible that the dimer-dimer interaction has the characteristics of a repulsive Yukawa interaction at long distances, since this is the functional form of the dimer wave function [35]. Therefore, we have considered a dimer-dimer interaction of the form

$$V(r) = V_G(r) \theta(R_g - r) + V_S(r) \theta(r - R_g) \theta(R_y - r) + V_Y(r) \theta(r - R_y), \quad (25)$$

where $V_G(r)$ is a Gaussian potential up to radial distance R_g , $V_Y(r)$ is a long-range repulsive Yukawa potential starting from radial distance of R_y , $V_S(r)$ is a cubic spline function, and θ

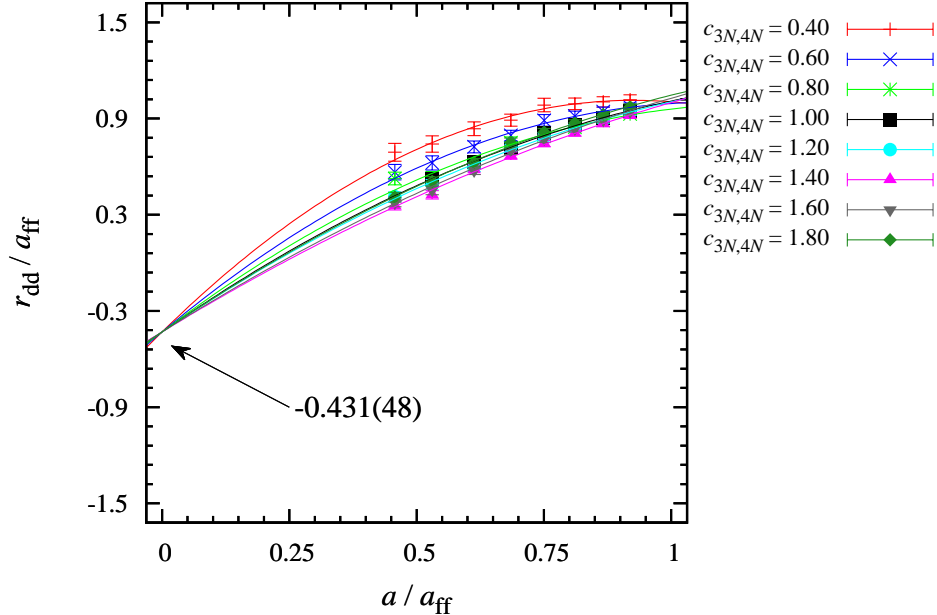


FIG. 6: The continuum-limit extrapolation of the dimer-dimer effective range r_{dd} . The final result is $r_{\text{dd}}/a_{\text{ff}} = -0.431(48)$.

is a unit step function. In all cases where the scattering length is positive, we find that the effective range is negative. We find that the repulsive Yukawa potential plays an important role making the effective range negative. These findings support our lattice result of a negative effective range for the dimer-dimer system and is also consistent with the negative value for the fermion-dimer effective range.

V. SUMMARY AND CONCLUSIONS

We have used lattice effective field theory to compute the scattering length and effective range of dimer-dimer scattering in the universal limit of large fermion-fermion scattering length. To benchmark our numerical lattice methods, we first calculated fermion-dimer scattering. The scattering phase shifts were computed by calculating finite-volume scattering energies and applying Lüscher's finite-volume method. In our calculations we included a three-particle interaction in order to generate additional data to be used in the continuum-limit extrapolations. The dependence on the three-particle interaction coefficient c_{3N} was consistent with the $(a/a_{\text{ff}})^{3.54544}$ dependence predicted by conformal scaling in the unitarity limit. Extrapolating to the continuum limit, we obtained the values $a_{\text{fd}}/a_{\text{ff}} = 1.176(6)$ and $r_{\text{fd}}/a_{\text{ff}} = -0.029(16)$, in excellent agreement with previous calculations of fermion-dimer scattering length and effective range.

We then used the same methods to calculate dimer-dimer scattering and extracted the dimer-dimer scattering length a_{dd} and effective range r_{dd} . In this case we used a multiparticle interaction coefficient $c_{3N,4N}$. We found that the finite-volume corrections could be reduced by making the three-particle interaction sufficiently repulsive. Using Lüscher's finite-volume method, we determined the dimer-dimer scattering phase shifts. We then extracted the values a_{dd} and r_{dd} and performed continuum-limit extrapolations. For the scattering length we obtained $a_{\text{dd}}/a_{\text{ff}} = 0.618(30)$, in good agreement with published results.

For the effective range we found $r_{\text{dd}}/a_{\text{ff}} = -0.431(48)$, which is different from previous estimates. However this new result represents the first calculation with quantified and controlled systematic errors.

Finally, we considered a simple model of the dimer-dimer system as two fundamental particles interacting via a short-range Gaussian interaction and a repulsive Yukawa potential to mimic the Pauli repulsion between identical particles. We found that the effective range is negative for cases where the scattering length is positive. This may explain why both the dimer-dimer and fermion-dimer effective ranges are negative.

Our results should have immediate applications to the universal physics of shallow dimers. One particularly useful application is in the determination of the ground-state energy density of a dilute gas of shallow dimers. The dimers behave as repulsive Bose particles, and the energy density has been determined up to order ρa_{dd}^3 [6–9] as well as the first correction proportional to $r_{\text{dd}}/a_{\text{dd}}$ [10]. This new value for the dimer-dimer effective range suggests that higher-order corrections to the energy density of a dilute gas of shallow dimers could be larger than previously thought.

ACKNOWLEDGMENTS

The authors are grateful for discussions with Yusuke Nishida and acknowledge partial support from the U.S. National Science Foundation grant No. PHY-1307453, the DFG (SFB/TR 110, “Symmetries and the Emergence of Structure in QCD”) and the BMBF (contract No. 05P2015 - NUSTAR R&D). The work of UGM was also supported in part by The Chinese Academy of Sciences (CAS) President’s International Fellowship Initiative (PIFI) grant no. 2017VMA0025. Computing resources were provided by the Higher Performance Computing centers at Mississippi State University, North Carolina State University and RWTH Aachen.

-
- [1] E. Braaten and H.-W. Hammer, Phys. Rept. **428**, 259 (2006) [cond-mat/0410417].
- [2] D. E. Gonzalez Trotter *et al.*, Phys. Rev. Lett. **83**, 3788 (1999). doi:10.1103/PhysRevLett.83.3788
- [3] H. Feshbach, Annals Phys. **19**, 287 (1962) [Annals Phys. **281**, 519 (2000)].
- [4] S. Inouye, M. R. Andrews, J. Stenger, H.-J. Miesner, D. M. Stamper-Kurn, W. Ketterle, Nature **392** 151 (1998).
- [5] W. Zwerger, ed., *The BCS-BEC Crossover and the Unitary Fermi Gas*, Lecture Notes in Physics, (Springer, 2012).
- [6] T. D. Lee and C. N. Yang, Phys. Rev. **105**, 1119 (1957).
- [7] T. D. Lee, K. Huang, and C. N. Yang, Phys. Rev. **106**, 1135 (1957).
- [8] T. T. Wu, Phys. Rev. **115**, 1390 (1959).
- [9] E. Braaten, A. Nieto, Eur. Phys. J. B **11**, 143 (1999).
- [10] E. Braaten, H. W. Hammer, and S. Hermans, Phys. Rev. A **63**, 063609 (2001) [cond-mat/0012043].
- [11] H. A. Bethe, Phys. Rev. **76**, 38 (1949).
- [12] P. F. Bedaque and U. van Kolck, Phys. Lett. B **428**, 221 (1998) [nucl-th/9710073].
- [13] J. W. Chen, G. Rupak and M. J. Savage, Nucl. Phys. A **653**, 386 (1999) [nucl-th/9902056].
- [14] D. S. Petrov, C. Salomon and G. V. Shlyapnikov, Phys. Rev. Lett. **93**, 090404 (2004).
- [15] D. S. Petrov, C. Salomon and G. V. Shlyapnikov, Phys. Rev. A **71**, 012708 (2005) [cond-mat/0407579 [cond-mat.stat-mech]].
- [16] J. P. D’Incao, S. T. Rittenhouse, N. P. Mehta and C. H. Greene, Phys. Rev. A **79**, 030501 (2009).
- [17] A. Bulgac, P. F. Bedaque and A. C. Fonseca, (2003), arXiv:cond-mat/0306302 [cond-mat].
- [18] G. Rupak, nucl-th/0605074.
- [19] P. Naidon, S. Endo and A. M. Garcia-Garcia, J. Phys. B At. Mol. Opt. Phys. **49** 034002 (2016).
- [20] J. von Stecher, C. H. Greene and D. Blume, Phys. Rev. A **76**, 053613 (2007).
- [21] D. Lee, Eur. Phys. J. A **35**, 171 (2008) [arXiv:0704.3439 [cond-mat.supr-con]].
- [22] D. Lee, Prog. Part. Nucl. Phys. **63**, 117 (2009) [arXiv:0804.3501 [nucl-th]].
- [23] S. Elhatisari, D. Lee, U. G. Meißner and G. Rupak, Eur. Phys. J. A **52**, no. 6, 174 (2016) [arXiv:1603.02333 [nucl-th]].
- [24] Y. Nishida and D. T. Son, Lect. Notes Phys. **836**, 233 (2012) doi:10.1007/978-3-642-21978-8_7 [arXiv:1004.3597 [cond-mat.quant-gas]].
- [25] Y. Nishida and D. T. Son, Phys. Rev. D **76**, 086004 (2007) doi:10.1103/PhysRevD.76.086004 [arXiv:0706.3746 [hep-th]].
- [26] M. Lüscher, Commun. Math. Phys. **105**, 153 (1986). doi:10.1007/BF01211097
- [27] M. Lüscher, Nucl. Phys. B **354**, 531 (1991).
- [28] C. Lanczos, J. Res. Nat. Bur. Stand. **45** 255 (1950).
- [29] S. Bour, S. König, D. Lee, H.-W. Hammer and U.-G. Meißner, Phys. Rev. D **84**, 091503 (2011) [arXiv:1107.1272 [nucl-th]].
- [30] F. Gabbiani, P. F. Bedaque and H. W. Griesshammer, Nucl. Phys. A **675**, 601 (2000) [nucl-th/9911034].
- [31] P. F. Bedaque, H. W. Hammer and U. van Kolck, Phys. Rev. C **58**, R641 (1998) [nucl-

- th/9802057].
- [32] P. F. Bedaque, G. Rupak, H. W. Griesshammer and H. W. Hammer, Nucl. Phys. A **714**, 589 (2003) [nucl-th/0207034].
 - [33] M. Lüscher, Commun. Math. Phys. **104** (1986) 177.
 - [34] D. Lee, Phys. Rev. B **75**, 134502 (2007) [cond-mat/0606706 [cond-mat.stat-mech]].
 - [35] D. S. Petrov, C. Salomon and G. V. Shlyapnikov, J. Phys. B: At. Mol. Opt. Phys. **38** (2005) S645-S660 [cond-mat/0502010 [cond-mat.stat-mech]].